Discontinuous Transitions and Rhythmic States in the D-Dimensional Kuramoto Model Induced by a Positive Feedback with the Global Order Parameter

X. Dai,[1,2,3] X. Li,[1,4,*] H. Guo,[1,2,3] D. Jia,[1,2,3] M. Perc,[5,6,7] P. Manshour,[8] Z. Wang,[1,2,†] and S. Boccaletti[3,9,10]
[1]*Center for OPTical IMagery Analysis and Learning (OPTIMAL), Northwestern Polytechnical University, Xi'an 710072, China*
[2]*School of Mechanical Engineering, Northwestern Polytechnical University, Xi'an 710072, China*
[3]*Unmanned Systems Research Institute, Northwestern Polytechnical University, Xi'an 710072, China*
[4]*School of Computer Science, Northwestern Polytechnical University, Xian 710072, China*
[5]*Faculty of Natural Sciences and Mathematics, University of Maribor, Koroška cesta 160, 2000 Maribor, Slovenia*
[6]*Complexity Science Hub Vienna, Josefstädterstraße 39, 1080 Vienna, Austria*
[7]*Department of Medical Research, China Medical University Hospital, China Medical University, Taichung 404, Taiwan*
[8]*Physics Department, Persian Gulf University, Bushehr 75169, Iran*
[9]*CNR—Institute of Complex Systems, Via Madonna del Piano 10, I-50019 Sesto Fiorentino, Italy*
[10]*Moscow Institute of Physics and Technology (National Research University), 9 Institutskiy per., Dolgoprudny, Moscow Region 141701, Russian Federation*

(Received 18 February 2020; revised 28 August 2020; accepted 1 September 2020; published 5 November 2020)

From fireflies to cardiac cells, synchronization governs important aspects of nature, and the Kuramoto model is the staple for research in this area. We show that generalizing the model to oscillators of dimensions higher than 2 and introducing a positive feedback mechanism between the coupling and the global order parameter leads to a rich and novel scenario: the synchronization transition is explosive at all even dimensions, whilst it is mediated by a time-dependent, rhythmic, state at all odd dimensions. Such a latter circumstance, in particular, differs from all other time-dependent states observed so far in the model. We provide the analytic description of this novel state, which is fully corroborated by numerical calculations. Our results can, therefore, help untangle secrets of observed time-dependent swarming and flocking dynamics that unfold in three dimensions, and where this novel state could thus provide a fresh perspective for as yet not understood formations.

DOI: 10.1103/PhysRevLett.125.194101

The raise of coordination from interactions among components of a system is ubiquitous in biological and social endeavors [1]. Synchronous patterns are indeed visible almost everywhere: from animal groups (bird flocks, fish schools, and insect swarms [1]) to neurons in the brain [2], and play a pivotal role in various functional aspects of real-world systems. Unraveling the essential mechanisms behind synchronization is therefore of great importance, and the Kuramoto model (and its various generalizations [3–6]) are the fundamental reference for the study of coupled phase oscillators giving rise to, among others, explosive synchronization (ES), Chimera, and Bellerophon states [7–12]. Almost all studies have so far concentrated on two-dimensional oscillators, whereas some physical problems need to be modeled by extending the Kuramoto model to higher dimensional spaces. Examples include the swarmalators moving in three-dimensional spaces, and the Heisenberg model in the sense of mean field [13–15].

On the other hand, a characteristic of many biological and social systems is the presence of positive feedback (PF) mechanisms between the coupling of the elementary constituents and the level of coherence in the system [16–19]. Of peculiar interest is plasticity, which leads to changes in the connection strength among individuals to achieve efficient global states, and which is observed in neuroscience (under the name of "Hebbian learning") [20] as well as in social science (under the name of "homophily") [21]. PF may lead the system to reach a fixed equilibrium state, or to attain a cyclic (rhythmic) dynamics. Here, by "rhythmic state," we refer to a macroscopic property of the system, where the global order parameter is time dependent and oscillates nearly periodically, rather than slightly vibrating around a fixed value due to finite-size effects. States in which a system periodically switches from one state to another are ubiquitous in nature [22]: rhythmic neural synchronization is observed, for instance, in the brain during several (cognitive or motorial) tasks and even at rest [23], and various observations point to periodic changes between synchronized and unsynchronized states in neuronal networks [24,25], which can be as slow as the unihemispheric sleep in some birds or marine mammals [26] or the so-called first-night effect in humans [27], or as fast as respiratory rhythm in various animals [28]. Cyclic movement activities within colonies of interacting ants [29] and the periodic dynamics of infectious diseases and

prey-predator interactions in populations [30] are other important examples of such rhythmic states in social networks.

In this Letter, we consider D-dimension Kuramoto model incorporating a PF mechanism (PFDDKM), which constitutes the generalization of the D-dimension Kuramoto model (DDKM) already considered by Chandra, Girvan, and Ott in Ref. [15]. Namely, in our model the coupling strength through which each phase oscillator interplays with all the others is positively correlated with the global order parameter. The result is that an oscillating state emerges spontaneously (and surprisingly) when D is odd, whereas the transition to synchronization displays always an explosive nature when D is even.

Let us then begin by considering an ensemble of N phase oscillators in the plane. Each oscillator's phase θ_i is ruled by

$$\dot{\theta}_i = \omega_i + \frac{\lambda}{N}\alpha_i \sum_{j=1}^{N} \sin(\theta_j - \theta_i), \tag{1}$$

where $i = 1 \cdots N$. ω_i and θ_i are, respectively, the natural frequency and the instantaneous phase of the ith oscillators, and λ is the overall coupling strength. In analogy with Ref. [31], the parameter α_i is here defined as the global coherence level in the system: $\alpha_i = R = |(1/N)\sum_{j=1}^{N} e^{i\theta_j}| \ \forall \ i = 1, \ldots, N$. In Eq. (1), the oscillator i is associated to the two-dimensional unit vector $\boldsymbol{\sigma_i} \in \mathbb{R}^{2\times 1}$ with components $(\cos\theta_i, \sin\theta_i)$, which obeys

$$\dot{\boldsymbol{\sigma_i}} = \mathbf{W}_i\boldsymbol{\sigma_i} + \frac{\lambda}{N} R \sum_{j=1}^{N} [\boldsymbol{\sigma_j} - (\boldsymbol{\sigma_j}\cdot\boldsymbol{\sigma_i})\boldsymbol{\sigma_i}], \tag{2}$$

with the 2×2 matrix $\mathbf{W}_i$ given by

$$\mathbf{W}_i = \begin{pmatrix} 0 & \omega_i \\ -\omega_i & 0 \end{pmatrix}. \tag{3}$$

In fact, Eq. (2) can be adopted for higher dimensions D, with fixing $\boldsymbol{\sigma_i} \in \mathbb{R}^{D\times 1}$, $\|\boldsymbol{\sigma}\| = 1$, and $\mathbf{W}_i$ being a real $D\times D$ anti-symmetric matrix with element ω_{jk}^i (for simplification, ω_{jk}^i are assumed to be independent identically distributed variables, unless otherwise stated). In all the rest of the Letter, the dimension D will refer, then, to the dimension of the vectors $\boldsymbol{\sigma_i} \in \mathbb{R}^{D\times 1}$. The order parameter will be now defined as $R = \|\boldsymbol{\rho}\|_t$, where

$$\boldsymbol{\rho} = \frac{1}{N}\sum_{i=1}^{N} \boldsymbol{\sigma_i}, \tag{4}$$

and $\|\cdot\|_t$ stands for the time average of the Euclidean norm.

When PF is absent (i.e., when $\alpha_i = 1, \ \forall \ i$), Ref. [15] already pointed out that the transitions to synchronization characterizing odd and even dimensions are different. Our simulations [32] are reported in Fig. 1, and unveil that PF is actually the source of a much richer scenario: the transition to synchronization is explosive (i.e., abrupt and discontinuous, like a first order phase transition) for all even dimensions, while at all odd dimensions it is mediated by a time-dependent rhythmic state. What is reported here at even dimensions extends the studies reported in Ref. [31], where it was pointed out that PF induces explosive synchronization (ES) for $D = 2$. On the other hand, the case of odd dimensions is remarkable, as R converges to constant values close to 0 or 1 for low and high values of λ, respectively, but in between the coherent and incoherent states R is time dependent and displays a rhythmic dynamics.

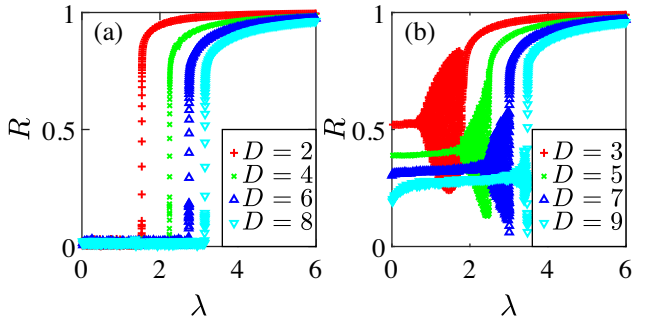

FIG. 1. The transition to synchronization. R vs λ (see text for definitions) for even D (a) and odd D (b). The used values of D are reported in the legends in both panels. $\omega_{jk}^i \sim U(-1, 1)$.

The observation of such a novel phenomenology induced us to perform several analytical studies, which are summarized here below. Due to space limitations, we here limited ourselves to give an account of the main results of our derivations, while the interested reader is addressed to the Supplemental Material [33] files where all details are reported.

The first step is to provide a static analytic prediction of the PFDDKM scenario at $D = 3$. In the limit of $N \to +\infty$, indeed, and following a similar approach as that used in Ref. [15], it is easy to verify (see [33] for all details) that when $\omega_{jk}^i \sim \mathrm{Norm}(0, 1)$ the order parameter satisfies $F(\lambda R, R) = 1$ [notice that for DDKM one has instead $F(\lambda, R) = 1$] where $F(\lambda, R)$ is defined as:

$$F(\lambda, R) = \frac{\lambda}{2}\int_{-1}^{1}\int_{-\infty}^{\infty} \frac{e^{-(\mu\lambda R)^2}/2}{(2\pi)^{3/2}} \times \sqrt{\frac{1-\mu^2+\sqrt{(\mu^2-2)^2+4\mu^2\xi^2}}{2}} d\xi d\mu. \tag{5}$$

Analogously, for $D = 2$, R satisfies $G(\lambda R, R) = 1$ [while for DDKM one would have $G(\lambda, R) = 1$], where $G(\lambda, R)$ is defined as

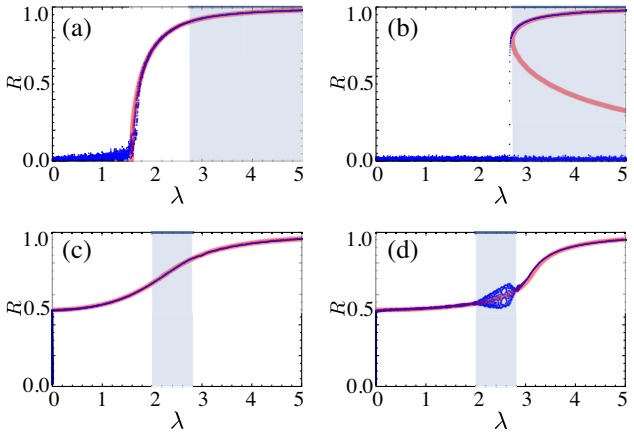

FIG. 2. Comparison between the DDKM and the PFDDKM models. R vs λ for (a) the DDKM at $D = 2$, (b) the PFDDKM at $D = 2$, (c) the DDKM at $D = 3$, (d) the PFDDKM at $D = 3$. The red curves are the solutions of Eqs. (5) and (6), the blue points are simulation results from Eq. (2) with $N = 5000$, and $\omega^i_{jk} \sim \mathrm{Norm}(0, 1)$. In the simulations of the forward (backward) transition, λ is gradually increased from 0 to 5 (is gradually decreased from 5 to 0) with steps $\delta_\lambda = 5 \times 10^{-6}$. The shadowed area is the hysteresis (unstable) region.

$$G(\lambda, R) = \lambda \int_{-1}^{1} \sqrt{1 - x^2}\, \frac{e^{-(\lambda R x)^2/2}}{\sqrt{2\pi}}\, dx. \tag{6}$$

A comprehensive comparison of DDKM and PFDDKM can therefore be drawn. In particular, Fig. 2 reports the solutions of Eqs. (6) and (6) together with the numerical simulations of Eq. (2). It is easy to see that the theoretical predictions are extremely accurate, and they even demonstrate that the introduction of PF at $D = 2$ [Fig. 2(b)] induces a first-order-like transition from coherence to incoherence. Yet, at this stage, the observed time-dependent (oscillatory) state is elusive [Fig. 2(d)], and therefore one needs to resort to other nonstatic methods.

Following the approach of Ref. [34], one can indeed obtain a reduced system. In that approach, one considers $\boldsymbol{\alpha}$ as being a real-valued D-dimensional vector such that $|\boldsymbol{\alpha}(\mathbf{W}, 0)| < 1$, and which satisfies the following equation

$$\frac{\partial \boldsymbol{\alpha}}{\partial t} = \frac{1}{2}(1 + \|\boldsymbol{\alpha}\|^2)\lambda R \boldsymbol{\rho} - \lambda R(\boldsymbol{\rho} \cdot \boldsymbol{\alpha})\boldsymbol{\alpha} + \mathbf{W}\boldsymbol{\alpha}, \tag{7}$$

where $\|\cdot\|$ is the Euclidean norm, until otherwise stated. It is easy to show (see [33] for full details) that, at $D = 3$, the order parameter is

$$\boldsymbol{\rho} = \int d\mathbf{W} G(\mathbf{W}) \hat{\boldsymbol{\alpha}}(\mathbf{W}, t) \Big[2\|\boldsymbol{\alpha}\|(1 + \|\boldsymbol{\alpha}\|^2) + (1 - \|\boldsymbol{\alpha}\|^2)^2 \log \frac{1 - \|\boldsymbol{\alpha}\|}{1 - \|\boldsymbol{\alpha}\|} \Big] \Big/ 4\|\boldsymbol{\alpha}\|^2, \tag{8}$$

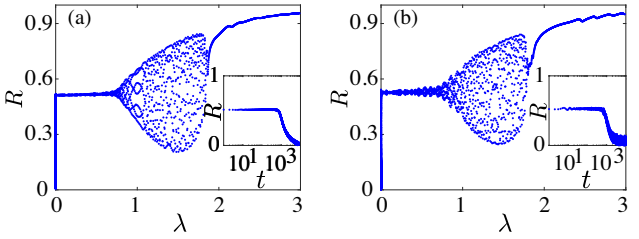

FIG. 3. Comparison between the full and the reduced systems. R vs λ at $D = 3$. λ is here gradually decreased from 3 to 0 with step $\delta_\lambda = 5 \times 10^{-6}$. (a) Simulation of the full system Eq. (2). (b) Simulation of the reduced system, from Eqs. (7) and (8). $\omega^i_{jk} \sim U(-1, 1)$. In both panels, the inset reports the time evolution of R at $\lambda = 0$.

where $G(\mathbf{W})$ is the probability density function (PDF) of $\mathbf{W}$. The hat notation indicates normalization: for $\boldsymbol{\alpha} \in \mathbb{R}^{n\times 1}$ one has $\hat{\boldsymbol{\alpha}} = \boldsymbol{\alpha}/\|\boldsymbol{\alpha}\|$.

While it is hard, in our case, to acquire a simpler representation of the reduced system (like the one obtained in Ref. [35]), one can still numerically simulate the dynamics of Eqs. (7) and (8). In particular, in Fig. 3 we report the results obtained for ω^i_{jk} sampled from a uniform distribution $U(-1, 1)$. Figure 3 compares the solution of Eq. (7) and Eq. (8) (for the integration of the reduced system, we used 7^3 equidistant samples of $\omega^i_{jk} \in [-1, 1]$) with that of the full system Eq. (2). One can see that the oscillatory states are now recovered by the reduction technique.

Going back to Fig. 1(b), one also sees that oscillations in R are not at all limited to the case $D = 3$. Rather, the backward phase transition diagrams at odd values of D display all the same feature: after a critical λ_B the system runs into an oscillatory state. In general, with D being larger, the system requires higher coupling strengths to sustain synchronized behaviors. For the case of D being odd, the oscillations in R affect the system for a shorter and shorter range of λ as D increases: as the critical order parameter $R_{\lambda_{0^+}}$ (R at λ_{0^+}) becomes smaller, the transition at higher D displays features similar to those of ES.

We now move to investigate the microscopic details behind the observed oscillations in R, and focus on the case $D = 3$, for which one can write $\mathbf{W}_i \boldsymbol{\sigma}_i = \boldsymbol{\omega}_i \times \boldsymbol{\sigma}_i$, where $\boldsymbol{\omega}_i$ has elements $(-\omega^i_{23}, \omega^i_{13}, -\omega^i_{12})$. Figure 4 illustrates the features of four typical system's phases in terms of four characteristic quantities: the local coherence $\phi_i = \boldsymbol{\rho} \cdot \boldsymbol{\sigma}_i / R$, the local coherence speed $\dot{\phi}_i$, the average speed $\langle \dot{\phi}_i \rangle$, and the standard deviation of the speed $\mathrm{std}(\dot{\phi}_i)$ (with averages being performed over 200 time steps). When compared to Fig. 3, the four phases displayed in Fig. 4 correspond to the following: uncoupled oscillators [$\lambda = 0$, Figs. 4(a1)–4(a4)], the initial plateau at $R \sim 0.5$ [$\lambda = 0.1$, Figs. 4(b1)–4(b4)], the oscillating state [$\lambda = 1.5$, Figs. 4(c1)–4(c4)], and the final fully coherent state [$\lambda = 2.0$, Figs. 4(d1)–4(d4)]. It is

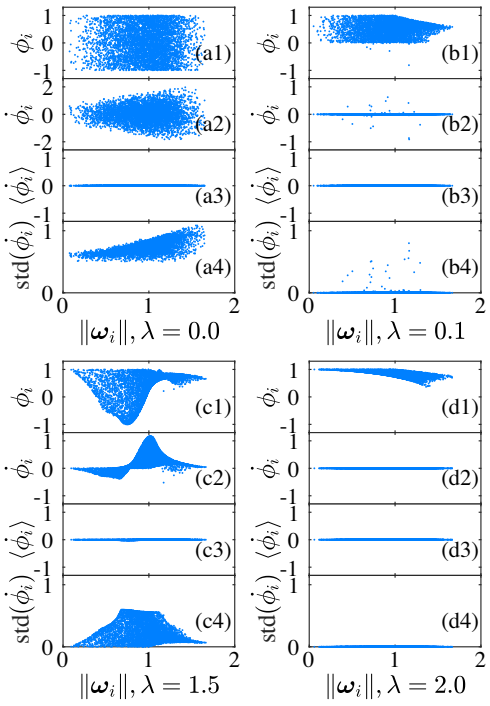

FIG. 4. Microscopic details of the observed rhythmic states. Snapshots at $t = 2 \times 10^4$ of the local coherence ϕ_i [(a1),(b1),(c1),(d1)], the local coherence speed $\dot{\phi}_i$ [(a2),(b2),(c2),(d2)], the average speed $\langle\dot{\phi}_i\rangle$ [(a3),(b3),(c3),(d3)], and the standard deviation $\mathrm{std}(\dot{\phi}_i)$ [(a4),(b4),(c4),(d4)] vs $\|\boldsymbol{\omega}_i\|$. See the main text for all definitions. $\omega^i_{jk} \sim U(-1, 1)$, $D = 3$ and the values of λ used in the simulations are reported in the bottom of each block of panels.

worth noticing that, in all cases, $\langle\dot{\phi}_i\rangle$ is almost vanishing, which means that each oscillator is fixed if averaged in time. Moreover, one sees that $\mathrm{std}(\dot{\phi}_i)$ is also almost vanishing for $\lambda = 0.1$ and $\lambda = 2.0$, which implies that oscillators are almost fixed on the sphere both in the final coherent state (as one could easily expect) and in the initial static plateau. ϕ_i and $\dot{\phi}_i$, instead, vary dramatically for $\lambda = 0$ and for $\lambda = 1.5$. Furthermore, at $\lambda = 0$ (i.e., for uncoupled oscillators), larger values of $\mathrm{std}(\cdot)$ characterize oscillators at larger $\|\boldsymbol{\omega}_i\|$, which indeed rotate faster along $\hat{\boldsymbol{\omega}}_i$ (here, $\hat{\boldsymbol{\omega}}_i = \boldsymbol{\omega}_i/\|\boldsymbol{\omega}_i\|$) with an angular frequency of $\|\boldsymbol{\omega}_i\|$.

Remarkably, this does not happen, instead, at $\lambda = 1.5$, i.e., when oscillations in R occur. There, one can see that those oscillators with middle $\|\boldsymbol{\omega}_i\|$ are the ones exhibiting larger values of $\mathrm{std}(\cdot)$, which is of particular interest because one could expect instead to have the oscillators with larger $\|\boldsymbol{\omega}_i\|$ unlocked. See [33] for more microscopic details of the oscillatory state at $\lambda = 1.5$.

The latter fact suggests to perform further microscopic investigations. Indeed, the probability density function (PDF) of speeds $\|\boldsymbol{\omega}_i\|$ considered so far is a unimodal function, implying that a large fraction of oscillators have

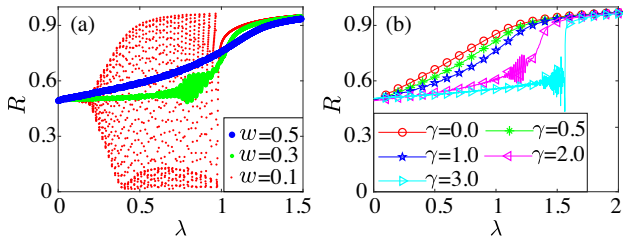

FIG. 5. The role of the probability density function of speeds. (a) R vs λ for $D = 3$, and different values of w. The speeds $\|\boldsymbol{\omega}_i\|$ are here sorted from a uniform distribution $U(d - w, d + w)$, with $\hat{\boldsymbol{\omega}}_i$ following an isotropic distribution $U(\hat{\boldsymbol{\omega}}_i)$ (see main text for all definitions). Once again, λ is gradually decreased from 1.5 to 0, with step $\delta_\lambda = 2 \times 10^{-6}$. The color code is reported in the legend. (b) R vs λ as it results from simulations of Eq. (1) with $\alpha_i = R^\gamma$, $D = 3$, and $w = 0.5$ (see text for definitions). The five used values of γ are reported in the legend.

middle frequencies. In order to investigate the role that different oscillators play in determining the rhythmic state, a uniform speed distribution $U_r(\boldsymbol{\omega}_i, d, w)$ is considered. This corresponds to sorting the speeds $\|\boldsymbol{\omega}_i\|$ from a uniform distribution $U(d - w, d + w)$, with $\hat{\boldsymbol{\omega}}_i$ following an isotropic distribution $U(\hat{\boldsymbol{\omega}}_i)$. This way, the limit $w \to 0$ corresponds to a narrow distribution, while in the limit $w \to d$, the PDF is wide and uniform. We then set $d = 0.5$, and study the effect of varying w. The results for $D = 3$ are reported in Fig. 5(a), and it is seen that wider ranges of $\|\boldsymbol{\omega}_i\|$ (i.e., larger w) are indeed able to remove the presence of the intermediate oscillatory states, and oscillations are almost vanishing for $w = 0.5$. The general conclusion is therefore that rhythmicity in the PFDDKM is strongly influenced by the properties (such as unimodality) of the PDF of the speeds $\|\boldsymbol{\omega}_i\|$.

The next interesting question is whether or not oscillatory states may occur for $w = 0.5$. To answer this point, we generalized our model and considered $\alpha_i = R^\gamma$ in Eq. (1), with γ being a real number. In Fig. 5(b), we report the simulations of the new system for $D = 3$, and one sees that the scenario is actually extremely rich: as γ increases, the transition can be continuous ($\gamma = 1.0$), mediated by the oscillatory state ($\gamma = 2.0$), or first-order-like ($\gamma = 3.0$).

Compared to other nonstationary states found in Kuramoto-like models, such as the Bellerophon state [10,36–39] (in which the oscillators form quantized clusters) or the Chimera state [40–42] (in which the oscillators form two groups, coherent and incoherent respectively), the rhythmic state observed in PFDDKM at odd dimensions appears to be essentially different. First, it conflicts with ES which is found at any even dimension. Second, it does not require bimodal distributions in the system's natural frequencies, as instead Bellerophon state does. Third, it is essentially due to large fluctuations of those oscillators with middle frequency.

Taken together, we have fully characterized the dynamics of a D-dimensional Kuramoto model in the presence of

an PF coupling. We have reported evidence that PF leads to explosive synchronization at all even dimensions of the model, thus generalizing previous results for $D = 2$. At odd dimensions, we have shown that the transition to synchronization is mediated by a time-dependent, rhythmic state that was not previously observed in coupled phase oscillators. Therein, the natural frequency plays a key role as oscillators are grouped spontaneously in three groups consisting of low, middle, and high frequency oscillators. We have also found two important conditions that affect the emergence of oscillations, namely the distribution of $\|\boldsymbol{\omega}_i\|$ and the introduction of PF. We have shown that distributions with a clear peak of $\|\boldsymbol{\omega}_i\|$ promote oscillations, as does the strength of PF. Importantly, the later condition is more important as it is the most fundamental difference between even and odd D.

Our research could find applicability in better understanding swarming and related collective phenomena in three dimensions [1], in particular where PF mechanism plays a key role, such as in fish schools or murmurations under predation [29,43].

We acknowledge support from National Natural Science Foundation of China (Grants No. 81961138010, No. U1803263, No. 11931015), and No. 61871470, Key Area R & D Program of Shaanxi Province (Grant No. 2019ZDLGY17-07), Key Area R & D Program of Guangdong Province (Grant No. 2019B010137004), the Fundamental Research Funds for the Central Universities (Grant No. 3102019PJ006), the seed Foundation of Innovation and Creation for Graduate Students in Northwestern Polytechnical University (Grant No. ZZ2019010), and the Slovenian Research Agency (Grants No. P1-0403 and No. J1-2457).

*Corresponding author.
li@nwpu.edu.cn
†Corresponding author.
zhenwang0@gmail.com

[1] T. Vicsek and A. Zafeiris, Phys. Rep. **517**, 71 (2012).
[2] W. Singer, Neuron **24**, 49 (1999).
[3] S. H. Strogatz, Physica (Amsterdam) **143D**, 1 (2000).
[4] J. A. Acebrón, L. L. Bonilla, C. J. P. Vicente, F. Ritort, and R. Spigler, Rev. Mod. Phys. **77**, 137 (2005).
[5] F. A. Rodrigues, T. K. D. Peron, P. Ji, and J. Kurths, Phys. Rep. **610**, 1 (2016).
[6] S. Boccaletti, J. Almendral, S. Guan, I. Leyva, Z. Liu, I. Sendiña-Nadal, Z. Wang, and Y. Zou, Phys. Rep. **660**, 1 (2016).
[7] Y. Moreno and A. F. Pacheco, Europhys. Lett. **68**, 603 (2004).
[8] I. Leyva, R. Sevilla-Escoboza, J. M. Buldú, I. Sendiña-Nadal, J. Gómez-Gardeñes, A. Arenas, Y. Moreno, S. Gómez, R. Jaimes-Reátegui, and S. Boccaletti, Phys. Rev. Lett. **108**, 168702 (2012).
[9] Y. Kuramoto and D. Battogtokh, Nonlinear Phenom. Complex Syst. **5**, 380 (2002).
[10] H. Bi, X. Hu, S. Boccaletti, X. Wang, Y. Zou, Z. Liu, and S. Guan, Phys. Rev. Lett. **117**, 204101 (2016).
[11] E. A. Martens, E. Barreto, S. H. Strogatz, E. Ott, P. So, and T. M. Antonsen, Phys. Rev. E **79**, 026204 (2009).
[12] S.-i. Shima and Y. Kuramoto, Phys. Rev. E **69**, 036213 (2004).
[13] J. Zhu, Phys. Lett. A **377**, 2939 (2013).
[14] K. P. O'Keeffe, H. Hong, and S. H. Strogatz, Nat. Commun. **8**, 1504 (2017).
[15] S. Chandra, M. Girvan, and E. Ott, Phys. Rev. X **9**, 011002 (2019).
[16] H. Kitano, Science **295**, 1662 (2002).
[17] P. J. Richerson and R. Boyd, *Not By Genes Alone: How Culture Transformed Human Evolution* (University of Chicago Press, Chicago, 2008).
[18] J. E. Ferrell, Jr., Curr. Opin. Cell Biol. **14**, 140 (2002).
[19] M. B. Diener and R. Milich, Journal of clinical child psychology **26**, 256 (1997).
[20] D. O. Hebb and D. Hebb, *The Organization of Behavior* (Wiley, New York, 1949), Vol. 65.
[21] M. McPherson, L. Smith-Lovin, and J. M. Cook, Annu. Rev. Sociol. **27**, 415 (2001).
[22] L. Glass and M. C. Mackey, *From Clocks to Chaos: The Rhythms of Life* (Princeton University Press, Princeton, 1988).
[23] G. Buzsaki, *Rhythms of the Brain* (Oxford University Press, Oxford, 2006).
[24] G. Buzsáki and W. Freeman, Curr. Opin. Neurobiol. **31**, v (2015).
[25] W. Freeman and R. Q. Quiroga, *Imaging Brain Function with EEG: Advanced Temporal and Spatial Analysis of Electroencephalographic Signals* (Springer Science & Business Media, New York, 2012).
[26] N. C. Rattenborg, C. Amlaner, and S. Lima, Neurosci. Biobehav. Rev. **24**, 817 (2000).
[27] M. Tamaki, J. W. Bang, T. Watanabe, and Y. Sasaki, Curr. Biol. **26**, 1190 (2016).
[28] D. H. Heck, S. S. McAfee, Y. Liu, A. Babajani-Feremi, R. Rezaie, W. J. Freeman, J. W. Wheless, A. C. Papanicolaou, M. Ruszinkó, Y. Sokolov *et al.*, Front. Neural Circuits **10**, 115 (2017).
[29] I. D. Couzin, Trends Cognit. Sci. **22**, 844 (2018).
[30] R. M. May, American Zoologist **25**, 441 (1985).
[31] X. Zhang, S. Boccaletti, S. Guan, and Z. Liu, Phys. Rev. Lett. **114**, 038701 (2015).
[32] Unless otherwise specified, our simulations refer to $N = 5000$. The differential equations are solved by a Runge-Kutta fourth-order method with integration time step $h = 5 \times 10^{-3}$. For tracking the transitions to synchronization, the parameter λ is increased and decreased by small steps of $\delta_\lambda = 5 \times 10^{-6}$, so that the evolution of R at different D is almost adiabatically tracked. Frequencies ω^i_{jk} are taken from a uniform distribution in the interval $(-1, 1)$.
[33] See the Supplemental Material at http://link.aps.org/supplemental/10.1103/PhysRevLett.125.194101 for a full account on the details of our analytical treatments.
[34] S. Chandra, M. Girvan, and E. Ott, Chaos **29**, 053107 (2019).

[35] E. Ott and T. M. Antonsen, Chaos **18**, 037113 (2008).
[36] T. Qiu, S. Boccaletti, I. Bonamassa, Y. Zou, J. Zhou, Z. Liu, and S. Guan, Sci. Rep. **6**, 36713 (2016).
[37] T. Qiu, I. Bonamassa, S. Boccaletti, Z. Liu, and S. Guan, Sci. Rep. **8**, 12950 (2018).
[38] C. Xu, S. Boccaletti, S. Guan, and Z. Zheng, Phys. Rev. E **98**, 050202(R) (2018).
[39] X. Li, T. Qiu, S. Boccaletti, I. Sendiña-Nadal, Z. Liu, and S. Guan, New J. Phys. **21**, 053002 (2019).
[40] D. M. Abrams and S. H. Strogatz, Phys. Rev. Lett. **93**, 174102 (2004).
[41] D. M. Abrams, R. Mirollo, S. H. Strogatz, and D. A. Wiley, Phys. Rev. Lett. **101**, 084103 (2008).
[42] M. R. Tinsley, S. Nkomo, and K. Showalter, Nat. Phys. **8**, 662 (2012).
[43] Y. Katz, K. Tunstrøm, C. C. Ioannou, C. Huepe, and I. D. Couzin, Proc. Natl. Acad. Sci. U.S.A. **108**, 18720 (2011).